AAS 99-443

NAVIGATING MARS GLOBAL SURVEYOR THROUGH THE MARTIAN ATMOSPHERE: AEROBRAKING 2

P. Esposito, V. Alwar, P. Burkhart, S. Demcak, E. Graat, M. Johnston and B. Portock
Jet Propulsion Laboratory, California Institute of Technology
4800 Oak Grove Drive
Pasadena, California 91109, USA
E-mail: Pasquale.B.Esposito@jpl.nasa.gov

The Mars Global Surveyor spacecraft was successfully inserted into an elliptical orbit around Mars on 9/12/97 with an orbital period of 45.0 hours. After two phases of aerobraking separated by a science-phasing-orbit interval, the orbital period was reduced to 11.6 hours on 3/27/98 and to 1.97 hours on 2/4/99. Aerobraking, through an uncertain Martian atmosphere, was responsible for circularization of the MGS orbit. Its correct termination led to a sun synchronous orbit with a local mean solar time near 2:03 am at the descending equator crossing.

This paper describes the second phase of aerobraking and: a) the estimation of an atmospheric density model for every drag pass or periapsis passage by analyzing doppler tracking data, b) the generation of short-term, that is over one to several orbits, accurate atmospheric density predictions, c) maintaining the spacecraft's orbit within upper and lower bounds of atmospheric density or dynamic pressure during each periapsis passage, and d) the prediction of accurate periapsis passage times (Tp) over one to fifteen orbits.

Finally, we summarize the post-aerobraking maneuvers and the state of the frozen, sun-synchronous, polar, MGS mapping orbit and its evolution.

MGS MISSION OVERVIEW AND CHRONOLOGY

An overview of the Mars Global Surveyor (MGS) mission is summarized in Table 1. As shown, the first phase of aerobraking (AB) covered approximately 6.5 months and 201 orbits during which the orbital period was reduced from 45.0 hours to 11.6 hours. The planning strategy and navigation analysis and flight operations have been summarized in Refs. 1 and 2. The second phase of AB covered approximately 4.5 months and 710 orbits; during this time, the orbit period decreased from 11.6 hours to 1.97 hours. After AB was completed, a short interval was devoted to continuous acquisition of doppler and range tracking data for Mars gravity field refinement and planning for the transfer to the mapping orbit maneuver (TMO). This established the initial, short period, polar, sun synchronous and frozen mapping orbit required for continuous MGS instrument observations. The mapping phase of the mission officially started on 3/9/99 and intensive and continuous acquisition of data from the five science investigations commenced. To date, two orbit trim

maneuvers (OTM) were executed, with a third being planned for 8/11/99, in order to refine the frozen orbit elements and maintain uniformly distributed ground tracks for the nadir pointed instruments.

Table 1

MARS GLOBAL SURVEYOR MISSION CHRONOLOGY

Event	Date (UTC, SCET)	Comment
Launch	11/07/96, 17:00:50	
TCM-1	11/21/96, 16:00	DV = 27.1 m/s *
TCM-2	03/20/97, 18:00	DV = 3.86 m/s
TCM-3	04/22/97, 00:00	Not executed
TCM-4	08/25/97, 16:17	DV = 0.29 m/s
Mars Orbit Insertion	09/12/97, 01:53:49	DV = 973.0 m/s Orbit period = 45.0 hours
First AB Phase		
Initiation maneuver	09/16/97, 17:58	AB-1 on A3; DV = 4.4 m/s
Hiatus orbits	10/13/97-11/7/97	Orbits 19 through 36
Termination maneuver	03/27/98, 08:57	ABX on A201; DV = 4.4 m/s
Science Phasing Orbits	03/28/98 to 09/22/98	Orbits 202 to 572
Solar Conjunction	05/13/98	
Second AB Phase		
Initiation maneuver	09/23/98, 17:52	AB-1 on A573; DV = 11.6 m/s
Termination maneuver	02/04/99, 08:02	ABX on A1284; DV = 61.9 m/s
Transfer To Initial Mapping Orbit		
Gravity calibration	02/04-19/99	Refine Mars gravity model
TMO Maneuver	02/19/99, 22:10	TMO on A1473+36 minutes DV = 22.0 m/s
Start Mapping Mission	03/09/99, 02:13	New orbit convention **
Deploy HGA (Orbit 247)	03/29/99	
OTM-1 (Orbit 729)	05/07/99, 14:44	DV = 3.54 m/s
OTM-2 (Orbit 1144)	06/10/99, 11:50	DV = 0.18 m/s
OTM-3 (Orbit 1905)	08/11/99	DV = 0.25 m/s; Planned

* DV = delta-velocity or magnitude of the velocity-change maneuver.

** Completed 1670 periapsis-orbits (orbit n defined from periapsis n to periapsis n+1). Start equator-crossing-orbits or mapping phase orbits (orbit n defined from descending equator crossing n to descending equator crossing n+1). Mapping orbit 1 started on 3/9/99; mapping orbit 1000 started on 5/29/99 with orbit 2000 to occur on 8/19/99.

NAVIGATION DURING THE SECOND PHASE OF MGS AEROBRAKING

Aerobraking Initialization

After the completion of the science-phasing-orbit (SPO) interval, the second phase of aerobraking was initiated by slowly decreasing the periapsis altitude and thus the spacecraft gently walked into the martian atmosphere. This procedure allowed us to determine the atmospheric density model at each periapsis altitude step and compare the results with predictions. Thus, systematic errors could be determined which would influence the walk-in procedure. This strategy was accomplished with the three aerobraking propulsive maneuvers (ABM) or velocity-changes, executed at apoapsis, as shown in Table 2. Also shown is the change in periapsis altitude (due to the ABM and the gravity field) and the navigation determined density and dynamic pressure at the periapsis passage after the execution of the maneuver.

Table 2

ABMs THROUGHOUT THE SECOND PHASE OF AEROBRAKING

ABM At Apoapsis An	Velocity-Change Magnitude (m/sec)	Periapsis Altitude At Pn; Pn+1 (km)	Atmospheric Density and Dynamic Pressure at Periapsis (kg/km^3; N/m^2)
WALK-INTO ATMOSPHERE			
573	11.61	171.1; 126.9	4.95; 0.052 at P574
574	0.36	126.9; 122.5	12.2; 0.13 at P575
576	0.18	122.6; 120.6	14.4; 0.15 at P577
MAIN AEROBRAKING PHASE			
580	0.18	121.5; 119.8	13.8; 0.15 at P581
582	0.18	119.9; 117.7	17.9; 0.19 at P583
615	0.15	114.0; 116.3	17.2; 0.18 at P616
622	0.07	115.6; 114.4	22.4; 0.23 at P623
632	0.07	114.0; 115.1	13.0; 0.13 at P633
635	0.07	113.1; 114.0	24.4; 0.25 at P636
641	0.13	114.6; 113.0	---
647	0.22	114.8; 112.0	29.9; 0.30 at P648
668	0.15	111.9; 113.7	19.5; 0.20 at P669
682	0.15	112.6; 113.4	33.7; 0.33 at P683
685	0.26	112.6; 115.2	---
710	0.12	113.1; 112.7	---
714	0.26	113.2; 114.2	26.0; 0.25 at P715
726	0.26	113.5; 114.0	27.9; 0.27 at P727
747	0.38	112.3; 114.5	15.1; 0.14 at P748
764	0.38	112.5; 115.3	11.9; 0.11 at P765
789	0.22	112.2; 113.3	16.5; 0.15 at P790
804	0.45	111.1; 113.9	14.7; 0.13 at P805
814	0.25	112.2; 114.5	14.4; 0.13 at P815
834	0.25	112.1; 112.7	31.9; 0.29 at P835
845	0.61	112.3; 115.2	19.2; 0.17 at P846

Table 2 (Continued)

ABMs THROUGHOUT THE SECOND PHASE OF AEROBRAKING

ABM At Apoapsis An	Velocity-Change Magnitude (m/sec)	Periapsis Altitude At Pn; Pn+1 (km)	Atmospheric Density and Dynamic Pressure at Periapsis (kg/km^3; N/m^2)
873	0.61	112.2; 116.3	6.03; 0.053 at P874
903	0.61	112.6; 116.8	6.23; 0.055 at P904
979	0.39	109.0; 111.2	10.2; 0.087 at P980
1000	0.69	108.7; 113.2	12.5; 0.10 at P1001
1069	0.19	107.5; 108.0	23.9; 0.19 at P1070
1203	0.60	100.4; 103.3	25.4; 0.18 at P1204
WALK-OUT OF ATMOSPHERE			
1214	1.1	103.3; 106.1	19.6; 0.13 at P1215
1238	1.0	107.9; 109.7	12.5; 0.083 at P1239
1256	1.0	109.9; 113.8	5.5; 0.036 at P1257
1269	0.4	114.0; 115.8	3.7; 0.024 at P1270
1284	61.93	116.7; 377.4	---

Aerobraking Main Phase - Orbit Circularization

The purpose of the main phase of AB was to circularize the orbit and reduce the orbital period to 1.97 hours. In addition, AB was to be terminated near 2/4/99 when the local mean solar time (LMST) at the orbital descending node was close to 2:00 am. This was to be accomplished while maintaining the orbit, during periapsis passage, within a dynamic pressure (or effectively density or altitude) corridor. The upper limit of the dynamic presure was set to guard against excessive pressure or force acting on the spacecraft's already damaged -X axis solar array yoke assembly. This limited the rate at which AB could be accomplished. The lower limit of the dynamic pressure corridor was set to insure that effective period reduction would occur on each orbit such that AB would terminate as scheduled.

The following models and astrodynamic constants were utilized by navigation at the beginning of the second phase of AB. Mars atmospheric density predictions were determined from Mars-GRAM (Mars Global Reference Atmospheric Model, Ref. 3) which was integrated into the flight operations software. A 50x50 Mars gravity field model, identified as JPL 50c, was adopted which represented the current state of Mars gravity analysis (Ref. 4). We adhered to the IAU'91 definition of Mars astrodynamic constants (Ref. 5), utilized the JPL Mars and satellite ephemerides identified as DE 403 and MAR033 respectively, and adopted the Mars reference surface for altitude calculations as the USGS reference spheroid (a=3393.4 km and f=0.005 2083).

Analysis and Atmospheric Density Model Estimation

From 9/23/98 to 2/4/99, MGS went through 710 orbits. For almost every periapsis-passage, the navigation team estimated an atmospheric density model based on the analysis

of two-way, coherent, doppler data and occasionally on one-way doppler with the spacecraft's ultra stable oscillator (USO) as the frequency reference. Note that for approximately one hour centered on periapsis passage, no doppler data could be acquired because MGS was in the drag attitude during which its high gain antenna could not be Earth pointed.

The acceleration model used to assess the result of the drag pass was the classical model which is dependent on the density (static, spherically symmetric, exponential model), spacecraft relative velocity, and spacecraft parameters such as the area-to-mass ratio and the drag coefficient (Ref. 2). With respect to the a priori density model, the base altitude was always chosen to be close to the actual periapsis altitude and the base density was generated from Mars-GRAM adjusted by a density factor described later.

The data acquisition and analysis strategy is schematically represented in Figure 1. The analysis epoch and initial conditions occur after the periapsis passage but before doppler data are acquired. Doppler data were acquired throughout the remainder of the orbit and extended at least one hour after the drag pass under analysis. In principle, data prior to periapsis passage are used to determine orbit elements and data after the drag pass determine orbit elements (especially the period and apoapsis altitude) modified by the passage through the atmosphere. From these differences, the atmospheric density model during periapsis passage is deduced. At the beginning of AB, one to two orbits were analyzed together; near the end of AB, multiple orbits (five to ten) were analyzed simultaneously. The data analysis procedure went as follows. First the initial conditions (epoch and spacecraft state) were generated from the previous analysis in which the last orbit overlapped the first orbit of the present analysis. The apriori one-sigma uncertainty was set at 10 km for the position and 1.0 to 0.1 m/s for the velocity components. Mars' gravity was initially modeled with the JPL 50c model; however, updates were generated using current MGS doppler data. This was especially important when the periapsis passage migrated to the southern polar region near the end of AB. Generally, the apriori gravity error model was that generated from the gravity field analysis. For each drag pass, a separate atmospheric density model was determined from the analysis of the two-way coherent doppler data. The scale height was fixed, the base altitude was set close to the the actual periapsis altitude and the base density was estimated. Usually, the apriori error on the base density was 100 percent of the nominal value. Finally, a post-periapsis impulsive velocity-change was estimated in order to account for spacecraft thrusting to maintain the drag pass attitude. Typical velocity estimates due to this perturbation were 10-20 mm/s.

Initially estimated parameters (typically a total of 40) were converged after 2-3 iterations; however, toward the end of AB, 4-7 iterations were necessary. Throughout this process, the doppler data were fit at or near their inherent noise level although on occasion small systematic trends were evident. Solution accuracy was monitored by a) review of the doppler and range residuals for systematic patterns even though the latter were not fit , b) assess that the estimated parameter changes were reasonable with respect to the nominal model and c) compare current and previous orbit propagations to establish consistency in predicted results.

Typical doppler residuals resulting from the above analysis are given in Figures 2 and 3. The first covers orbit 577 (9/25/98) when the orbital period was 11.5 hours. There are 550 doppler with a count time of 60 seconds and a sigma of 3.35 millihertz or 0.060 mm/sec in range-rate. For these orbits, the range data was biased by 24 meters which was due to the Mars ephemeris. The second figure covers orbits 1053 to 1060 (1/12,13/99)

when the period was 3.0 hours. There are 623 doppler with a count time of 60 seconds and a sigma of 2.17 millihertz or 0.039 mm/sec in range-rate.

Throughout AB the reconstructed atmospheric density models are summarized in Figure 4. The atmospheric density scale height, H, was held constant for a large number of orbits until consultation with our atmospheric advisory group indicated that a change was advisable. Thus, H was 13 km for P573, 6.5 km for P574-P866, 7.0 km for P867-1052 and 6.0 km for P1053-P1284. Primarily because the AB corridor was specified in dynamic presure, we include Figure 5 which gives the navigation reconstruction of dynamic pressure throughout AB. Aerobraking progress is summarized in the period reduction (Figure 6) and the period-change per orbit (Figure 7). Finally, periapsis and apoapsis altitudes (hp and ha) are shown in Figure 8. The hp variation was responsible for maintaining the spacecraft within the dynamic pressure corridor. Discontinities in the trend are due to the execution of ABMs as given in Table 2. As indicated, most of the ABMs caused hp to increase since there was a natural drift toward decreasing periapsis altitudes.

Note that while we stress the navigation analysis and flight operations procedures, a related paper, Ref. 6, gives the AB planning and strategy development.

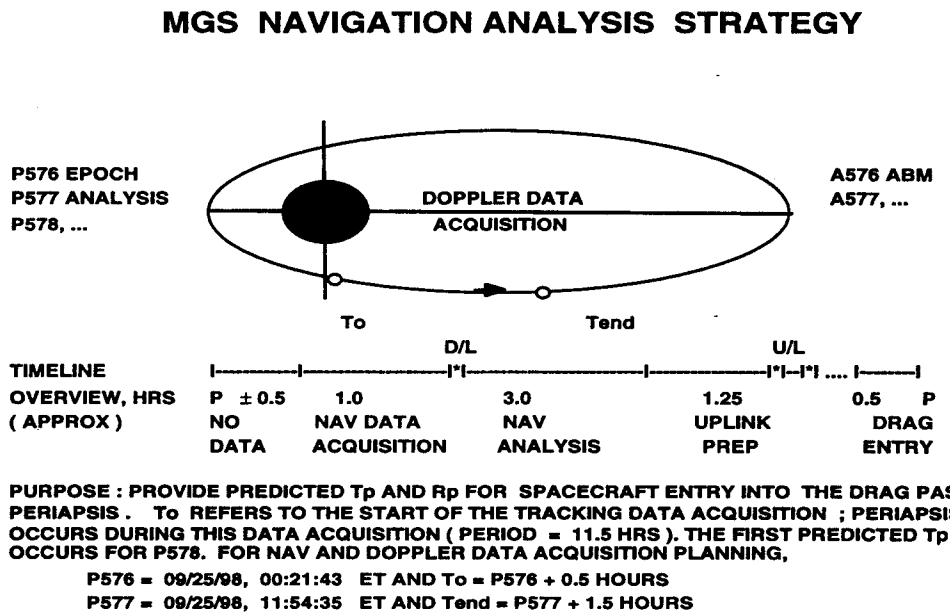

Figure 1 Overview Of Navigation Data Acquisition And Analysis Strategy

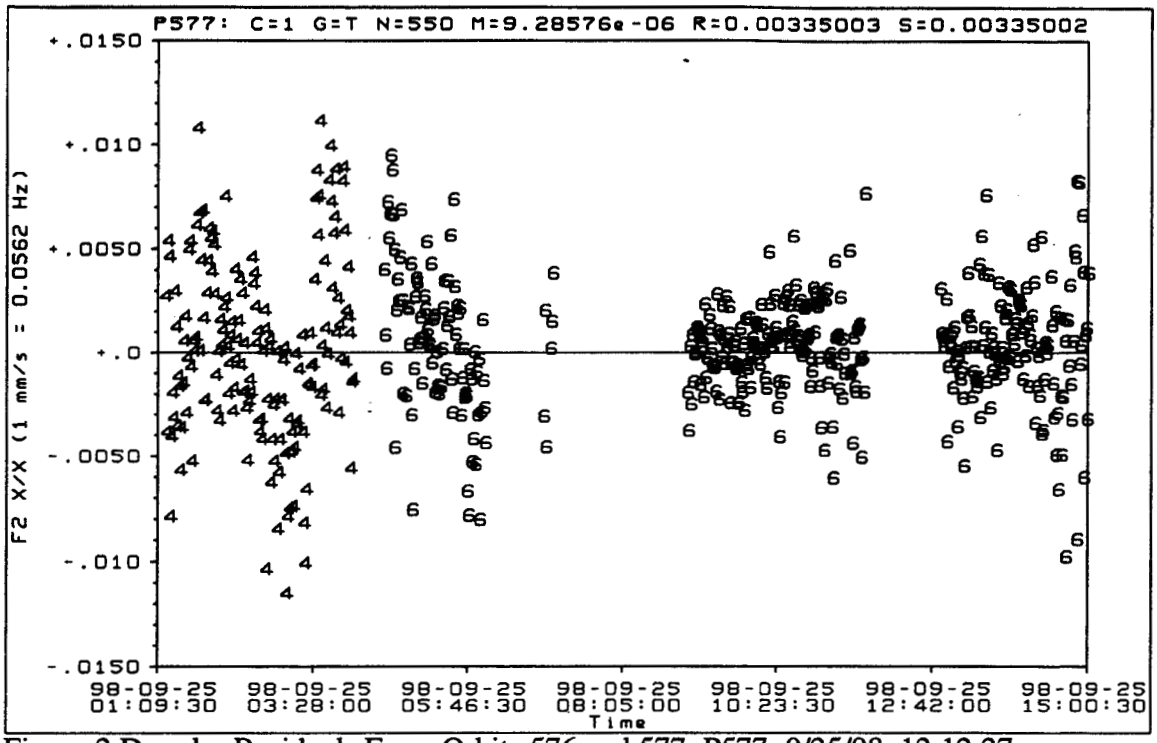

Figure 2 Doppler Residuals From Orbits 576 and 577; P577=9/25/98, 12:12:27

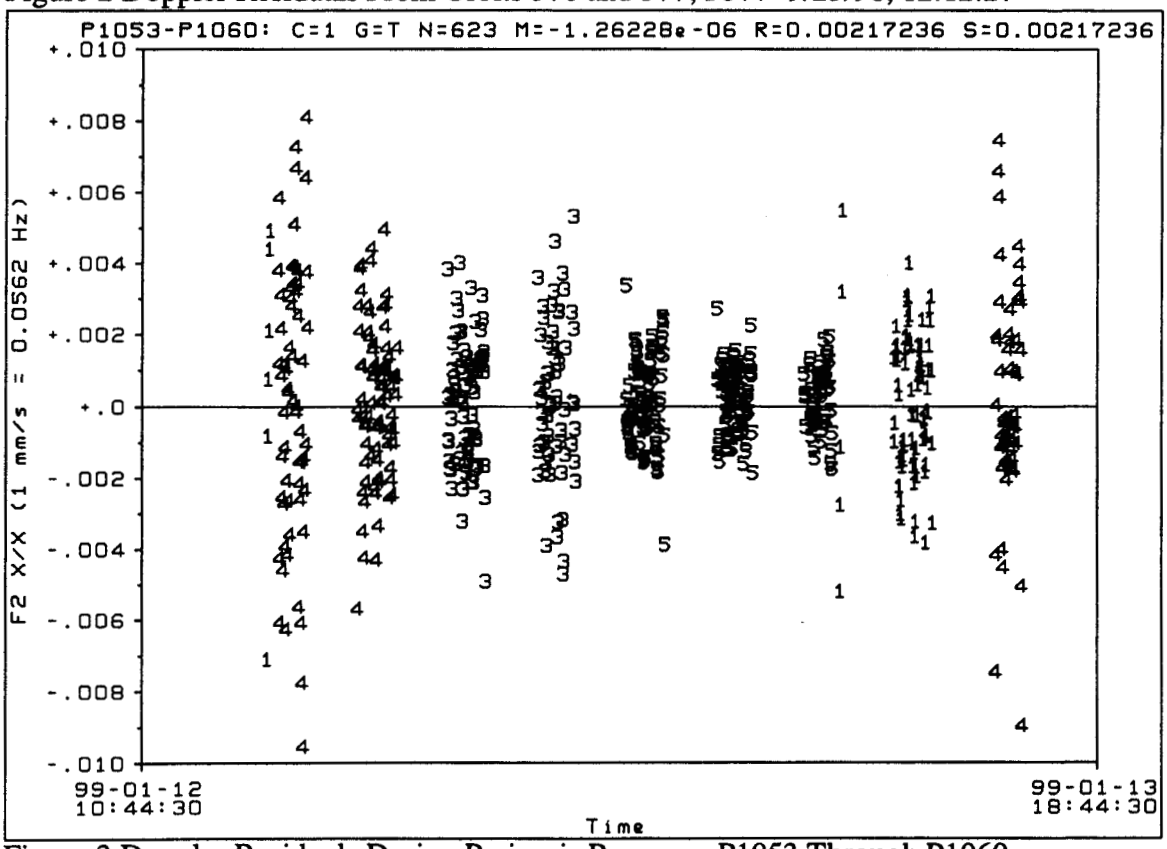

Figure 3 Doppler Residuals During Periapsis Passages, P1053 Through P1060

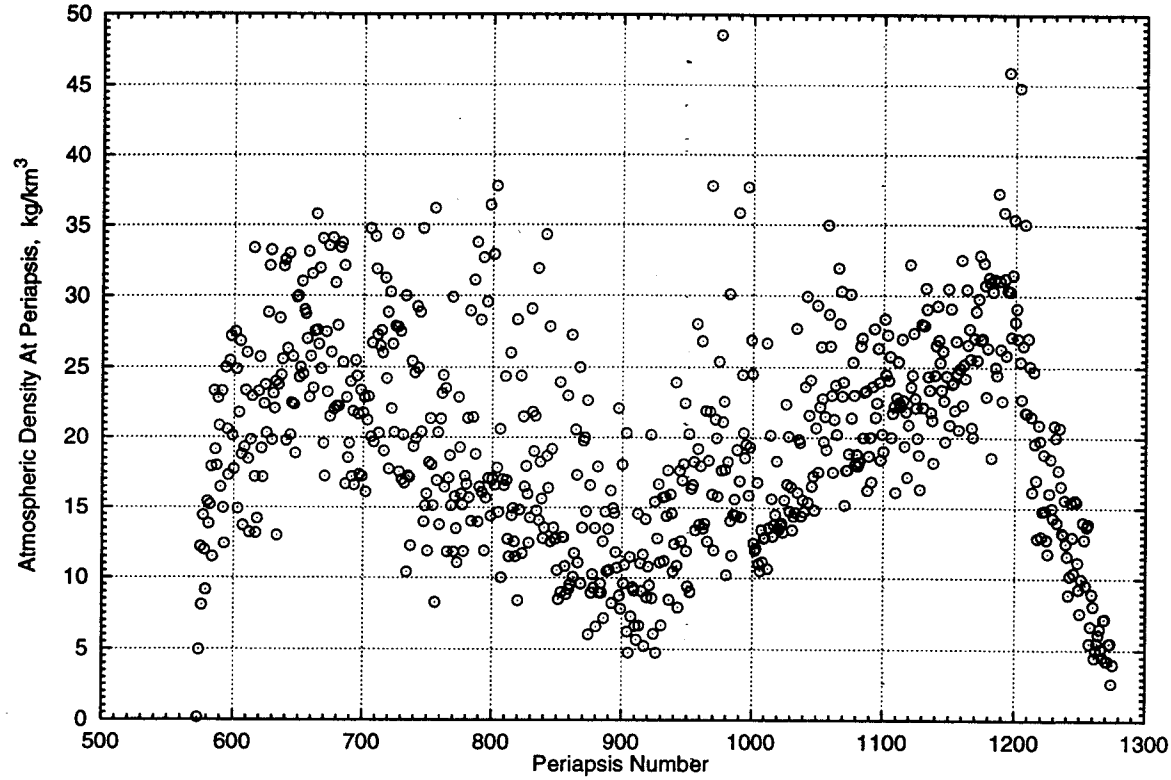

Figure 4 Atmospheric Densities At Periapsis Passage Determined For Almost 700 Drag Passes

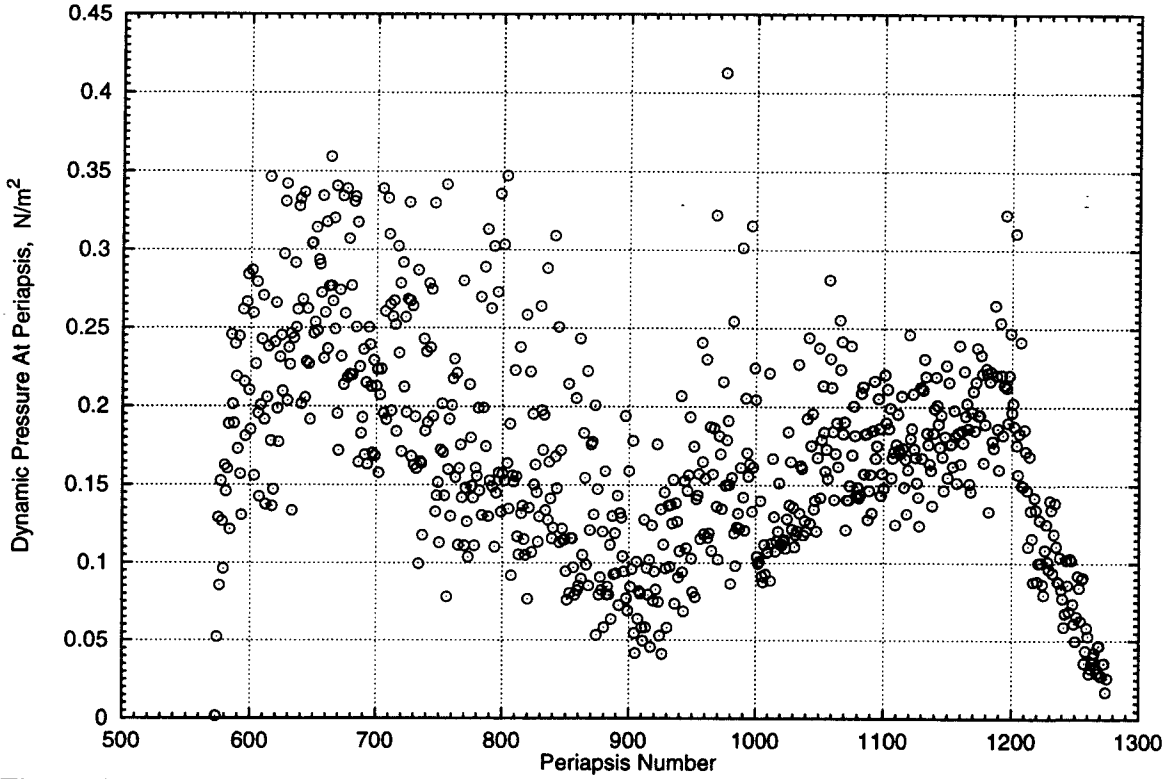

Figure 5 Dynamic Pressure Variation, At Periapsis Passage, Throughout Aerobraking

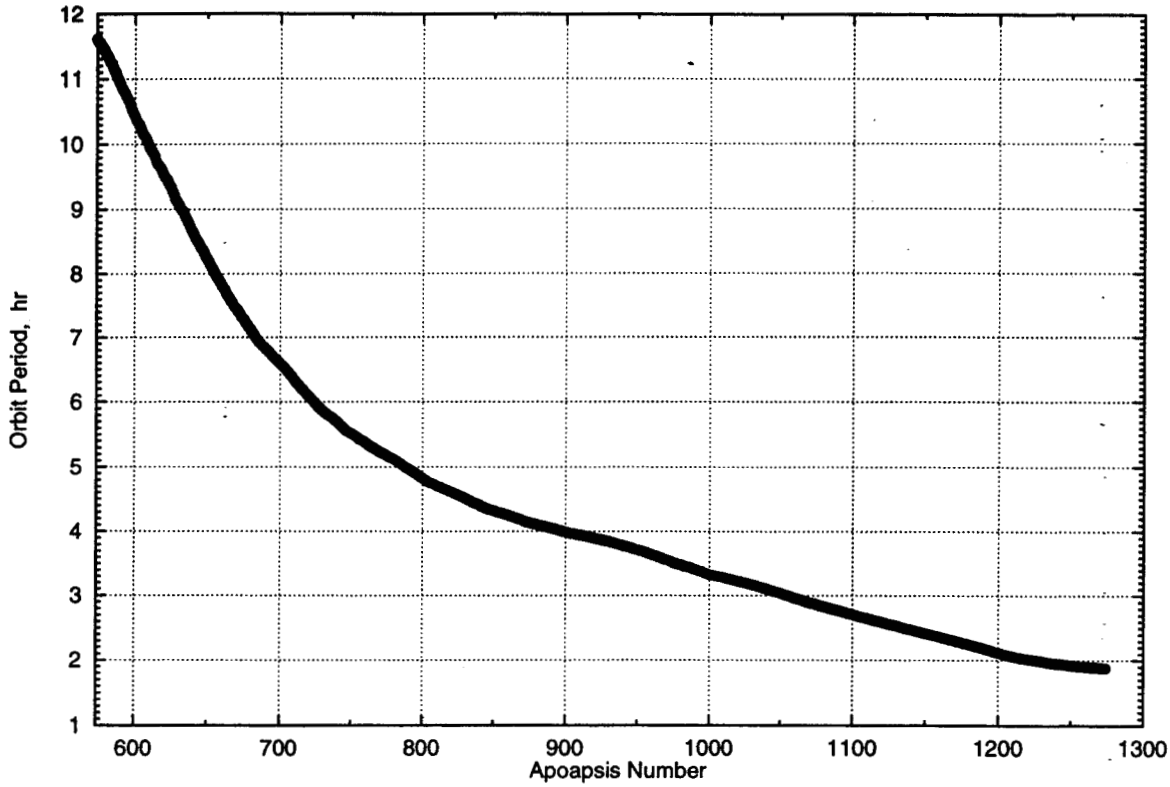

Figure 6 Orbit Period Reduction Throughout Aerobraking

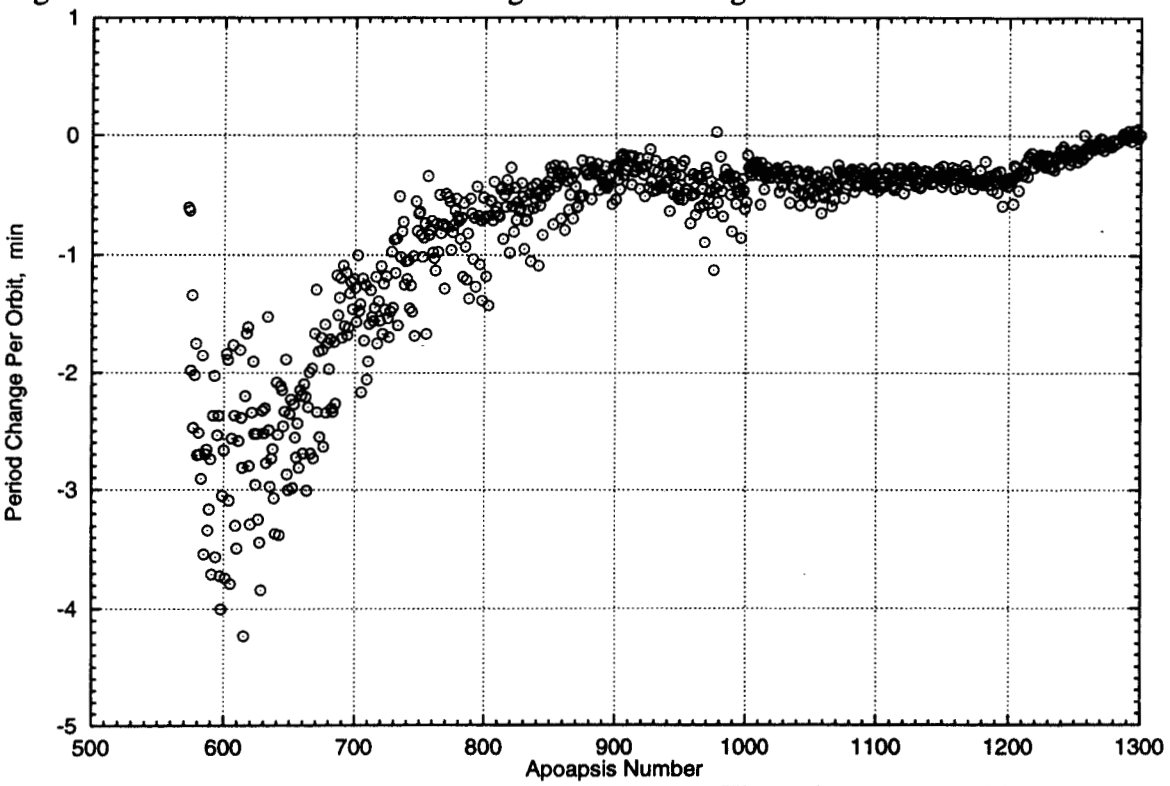

Figure 7. Orbit Period Reduction Per Periapsis Passage Throughout Aerobraking.

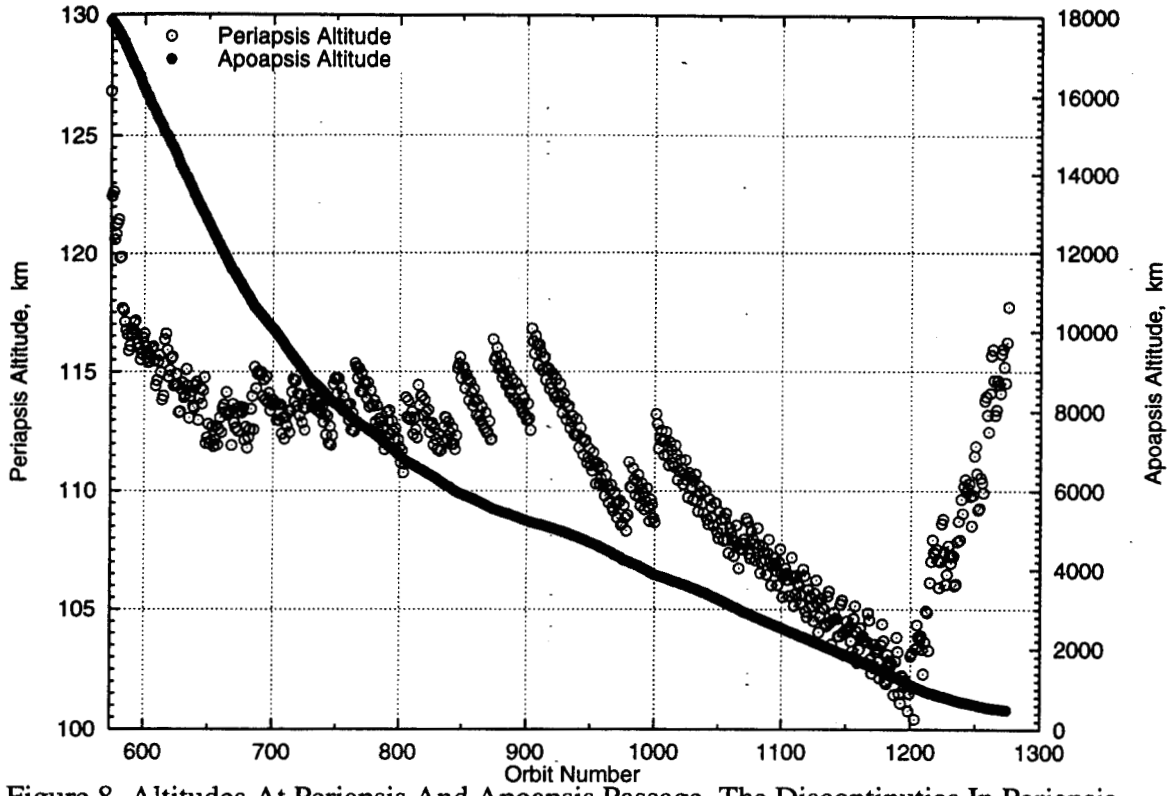

Figure 8 Altitudes At Periapsis And Apoapsis Passage. The Discontinuties In Periapsis-Altitudes Are Due To The Execution Of A Propulsive Maneuver At The Previous Apoapsis In Order To Keep Densities Or Dynamic Pressures Within Safe And Effective Limits

Atmospheric Density Waves And Density Predictions

An important trend in the reconstructed atmospheric density at periapsis was established when plotted against the longitude (east) of the periapsis passage location. An example of this nearly periodic trend is given in Figure 9. This figure was constructed by calculating the ratio of the navigation reconstructed density and the density predicted by the Mars-GRAM program for the same physical conditions; thus, a density factor (F) was established as

$$F = \frac{\text{density (reconstructed from navigation analysis)}}{\text{density (Mars-GRAM prediction)}} . \qquad (1)$$

Since this trend exhibited periodic behavior, it was fitted to a truncated fourier series of the form

$$F = F_o + \Sigma F_n \cos (n\lambda - \phi_n); \quad n=1,2,3,4. \qquad (2)$$

The fitted parameters were the non-dimensional factors, Fn, and the phases, ϕn, with the east longitude of the periapsis passage location denoted as λ. As shown in Figure 9, there are 63 measured values of F corresponding to periapsis-passages P574 through P636 occurring from 9/24/98 to 10/20/98. The values corresponding to the best fit curve are

given in Table 3. Note that the value of the bias term is 2.49 and therefore, Mars-GRAM is under-predicting the density. Also the amplitude of the fitted curve varies from 3.05 near 100 deg to 1.8 near 170 deg longitude; this is a factor of 1.7 density variation over 360 deg in longitude. Initially, this trend was observed consistently, with only minor variation over time. Thus, we corrected the Mars-GRAM predicted density over approximately one week intervals by the following equation

$$\rho(\text{updated}) = F \cdot \rho(\text{Mars-GRAM}) \qquad (3)$$

which was then applied to the drag acceleration model in the navigation software. This procedure enabled a significant improvement in predicted densities based upon what was observed in the recent past. Better density predictions rippled through the entire navigation prediction process. This was a key element in the successful implementation of MGS aerobraking.

Table 3

DENSITY FACTOR FUNCTION RESULTS

Index	Amplitude, Fn	Phase ϕ, deg
0	2.493	---
1	0.141	18.97
2	0.136	175.62
3	0.462	328.17

In Figure 10, we give three density factor functions, resulting from the above process, which occurred toward the end of AB. As indicated, the stable trend noted previously became less reliable when the periapsis passage drifted past the equator into the southern hemisphere and then over the southern polar region. The density data used to calculate these density functions came from: a) periapses 821-902 (12/7-21/98) for the solid curve, b) periapses 907-945 (12/22-28/98) for the dashed curve and c) periapses 944-978 (12/28/98 to 1/2/99) for the lower dashed curve.

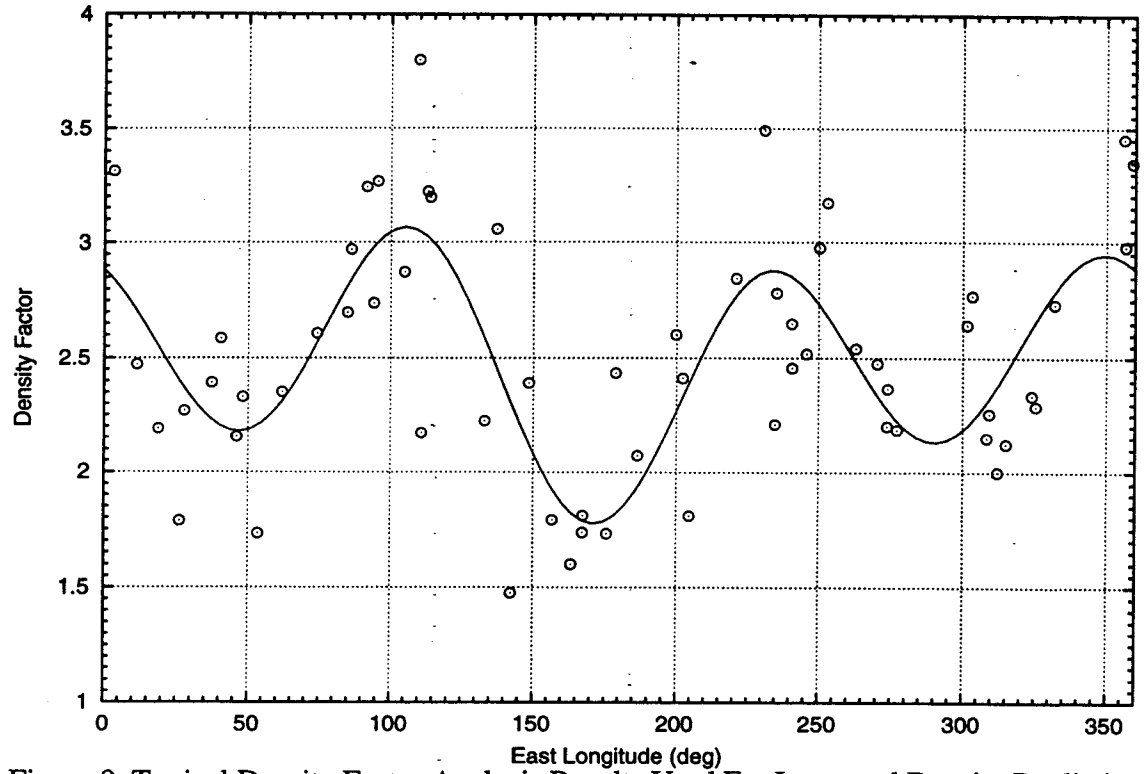

Figure 9 Typical Density Factor Analysis Results Used For Improved Density Prediction

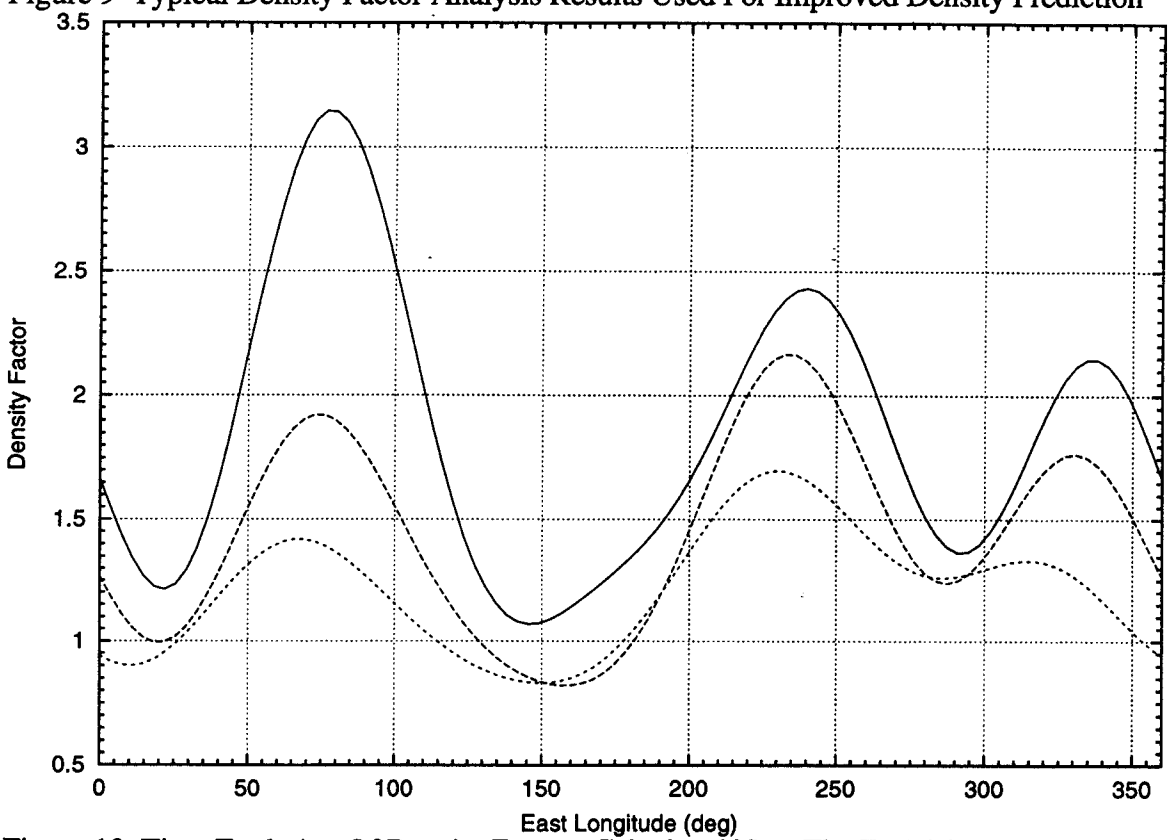

Figure 10 Time Evolution Of Density Factors Calculated Near The End Of Aerobraking

Orbit Predictions

Previously, we described the process of improving the atmospheric density prediction (or equivantly the dynamic pressure) which was essential for maintaining the spacecraft within the dynamic pressure corridor. The decision to execute an ABM, by specifying the apoapsis and velocity-change, was a function of the predicted density and dynamic pressure. Accurate predictions meant that ABM parameters could be specified with confidence and early enough to establish a reasonable planning and implementation cycle. Poor predictions would lead to uncertainty in the ABM selection and execution time.

In addition to ABM planning, accurate predictions of the time of periapsis passage, Tp, were necessary because the spacecraft's execution of its sequence of events were all relative to Tp. For example, the spacecraft's entry to and exit from the drag pass as well as maintaining the drag pass attitude were referenced to the predicted Tp. Unacceptable errors in the Tp predictions would cause systematic errors in the spacecraft's attitude and unnecessary thruster firings to maintain that attitude. The requirement on navigation was to predict Tp within 225 sec and 280 sec at the beginning and end of AB respectively. The number of predicted orbits or Tps satisfying the requirement per navigation analysis was directly dependent on the accuracy of the density prediction and the expected period change resulting from the drag pass. Our assumption at the beginning of AB was to be prepared for intrinsic, orbit-to-orbit density variations of 70 percent of the expected density in addition to the density variation associated with altitude variation.

The first predicted Tp, resulting from a navigation analysis, was generally accurate to 0.01-0.05 sec except near the end of AB when the periapsis passage location migrated to the southern polar region. There the accuracy degraded by a factor of 5-10 due to larger gravity field model uncertainty. The accuracy of the second Tp prediction varied depending on the estimate of the density and period reduction on the previous periapsis passage. In general, the predicted accuracy of the nth Tp depended on the accumulated effect of the previous n-1 periapsis passages and the errors associated with the predicted densities. A summary of the errors of the second Tp prediction resulting, from a series of navigation analyses, is given in Figure 11. These errors were constructed by a) differencing Tp(reconstructed for orbit n) and Tp(reconstructed for orbit n-1 but predicted one orbit ahead to orbit n) for the first Tp prediction, b) differencing Tp(reconstructed for orbit n) and Tp(reconstructed for orbit n-2 but predicted two orbits ahead to orbit n) for the second Tp prediction, and so on.

Toward the end of AB, the expected period change per orbit was quite small and thus many predicted Tps per navigation analysis would satisfy the requirement. On the other hand, many accurate Tp predictions were necessary because the period was approaching two hours and the command uplink process (i. e. orbit determination, command generation and transmission processes) were taking 5-6 hours. A representative summary of the accuracy of the Tp predictions near the end of AB, for five separate navigation analyses, is given in Figure 12. This covers orbits 950 to 1000 (12/29/98 to 1/4/99) when the period was 3.0 hours. This figure shows the rate of Tp error growth per analysis. For example, doppler data for orbits 950 to 952 were analyzed and predicted Tps for the next fifteen orbits were generated starting with Tp(953). Later, doppler data for all fifteen orbits were analyzed resulting in reconstructed Tps whose accuracy was at the level of 0.01 sec. For this case, 14 Tp predictions are within 280 sec. A positive error means that the predicted Tp is too early. This trend is a function of the accuracy and sign of the density predictions throughout the prediction interval. As shown, the error growth is generally quadratic.

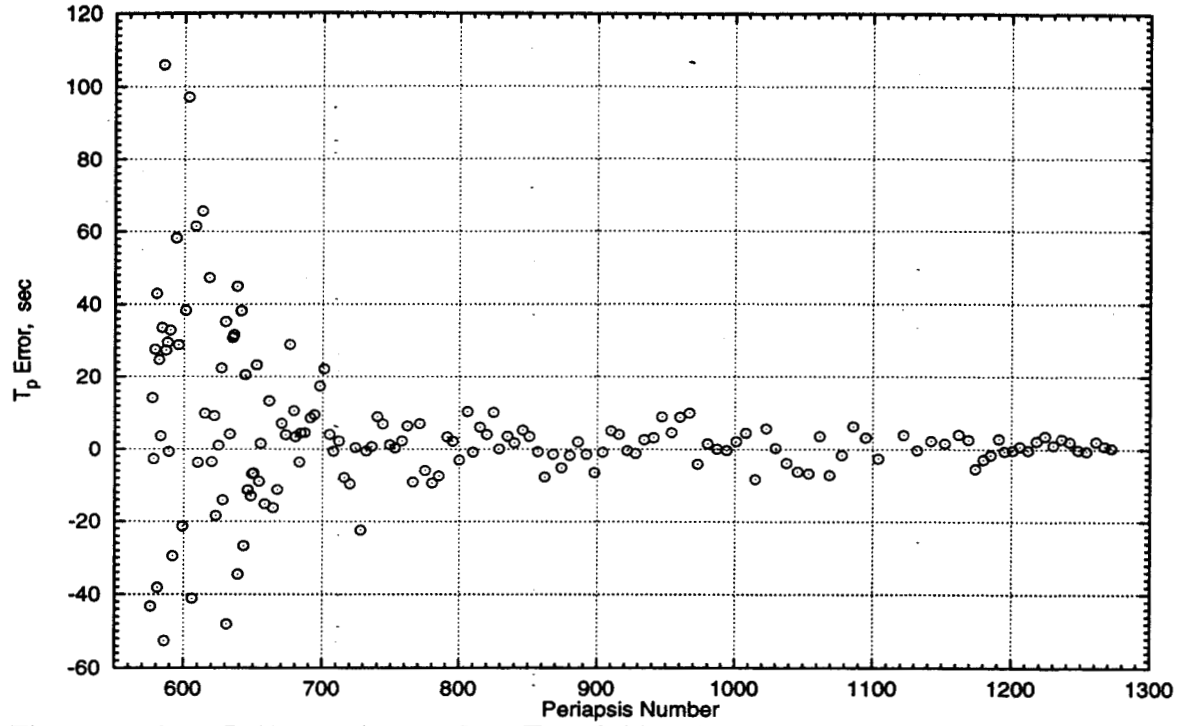

Figure 11 Error In Tp Predictions Over Two Orbits Throughout Aerobraking

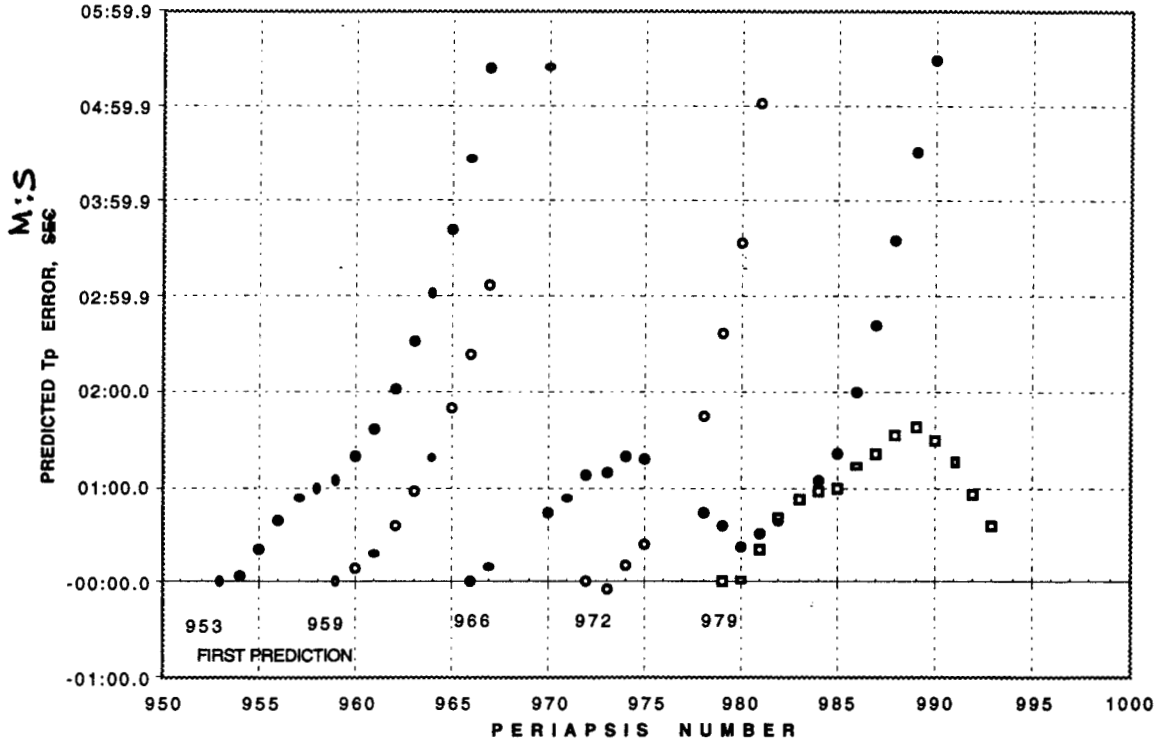

Figure 12 Error Propagation In Tp, For Multiple Predictions, For Five Separate Navigation Analyses. Results Of The First Analysis, Indicated By The First Prediction Tp(953), Show That Fourteen Tp Predictions Would Satisfy The 280 sec Accuracy Requirement

Aerobraking Termination

On 2/4/99 at A1284, after a brief walk-out of the atmosphere and series of maneuvers shown in Table 2, a propulsive maneuver to take the spacecraft out of the sensible atmosphere was performed. The maneuver targets and achieved orbit are shown in Table 4.

Table 4

AEROBRAKING TERMINATION MANEUVER, ABX TARGETS AND RESULTS

Orbit Element	Target	Achieved
Periapsis Altitude (P1285), km	381.0	377.4
Apoapsis Altitude (A1285), km	450.0	454.3

Altitudes Prior To The ABX Maneuver On Orbit 1284
Periapsis Altitude (P1284), km = 116.7
Apoapsis Altitude (A1284), km = 456.5

ACHIEVING THE MGS MAPPING ORBIT

Almost two weeks after completing AB, the execution of the transfer to the initial mapping orbit maneuver (TMO) was accomplished with the targets and achieved results shown in Table 5. This event was a milestone in the life of the MGS project and was the successful culmination of intense project activities which started at MOI. The remaining major event was to deploy the spacecraft's high gain antenna (HGA) and thereafter acquire continuous science observations over one Mars year.

Table 5

TRANSFER TO THE INITIAL MAPPING ORBIT MANEUVER* TARGETS AND RESULTS

Orbit Element (Periapsis)	Ideal Targets Initial Frozen Orbit	TMO Design P1474	Achieved Results P1474
Semi-major axis, km	3766.7	3766.7	3767.1
Eccentricity	0.00626	0.00623	0.00624
Arg of Periapsis, deg	270.0	269.2	268.7
hp, km	---	367.4	367.8
ha, km **	---	438.3	438.5

* TMO targets specified at periapsis 1474 (02/19/99, 22:50:33 UTC,SCET); this maneuver started at A1473 + 36 minutes.
** at apoapsis

The official start of the mapping mission began on 3/9/99 and for almost twenty days observations were made in a fixed HGA mode as a precaution to unexpected HGA deployment problems. On 3/29/99, the HGA was successfully deployed and MGS was fully functional and operational.

Mapping Orbit Evolution and Orbit Trim Maneuvers (OTM)

At the start of the mapping phase, the requirements on the orbit were: polar, sun-synchronous at 2:00 am at the descending node, short period and frozen. The reconstructed, osculating orbit elements at this epoch are given in Table 6.

Table 6

ORBIT ELEMENTS AT THE START OF MAPPING PHASE

Element	Periapsis Value	Apoapsis Value
Semi-major axis, km	3767.096	3767.541
Eccentricity	0.00548	0.0115
Inclination, deg	92.908	92.930
Arg of Periapsis, deg	264.878	261.818
Long of Ascend Node, deg	7.971	7.995
Epoch, 3/9/99, ET	02:41:35	03:39:24
Period, min	117.0	117.02
LMST, h:m:s *	02:02:46	

Mars centered, Mars mean equator of date and Earth mean equator of epoch J2000
* At the descending equator crossing

Figures 13, 14, and 15 summarize key parameters in the evolution of the mapping orbit. The LMST exhibits a slow drift of -1 minute over 1400 orbits and is easily within the allowable tolerance of ±12 minutes. Altitudes at periapsis and apoapsis are nearly constant as shown. The OTM executed on orbit 729 decreased this variation as indicated. Figure 15 gives the evolution of eccentricity and argument of periapsis and thus the degree of "frozen orbit" achieved. The outer trend shows the variation until the execution of the OTM-1; the inner trend reflects the effect of this maneuver and the success in refining the frozen orbit. The original concept for applying a frozen orbit to this mission is given in Ref. 7.

Perhaps the most interesting figure is the ground-track walk (GTW) evolution as given in Figure 16. This "walk" occurs over 88 orbits and is defined as the longitude difference between orbit n and orbit n-88 at the descending equator crossing. The ideal walk interval is 58.6 km eastward and that achieved at the start of mapping was 27.8 km eastward. This walk is very sensitive to small perturbations, especially to spacecraft self-induced effects. For example, angular momentum desaturations (AMD) effectively impart a small, but noticeable velocity perturbation to the orbital motion.

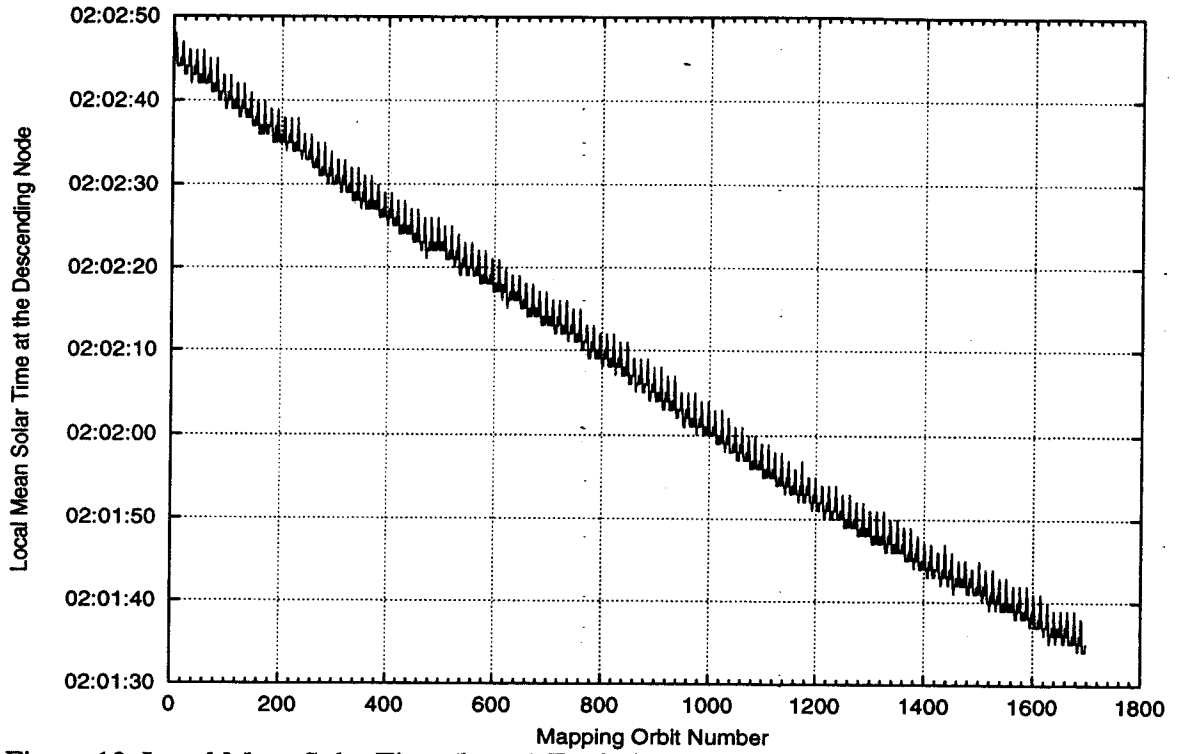

Figure 13 Local Mean Solar Time (h:m:s) Evolution Throughout The Mapping Phase

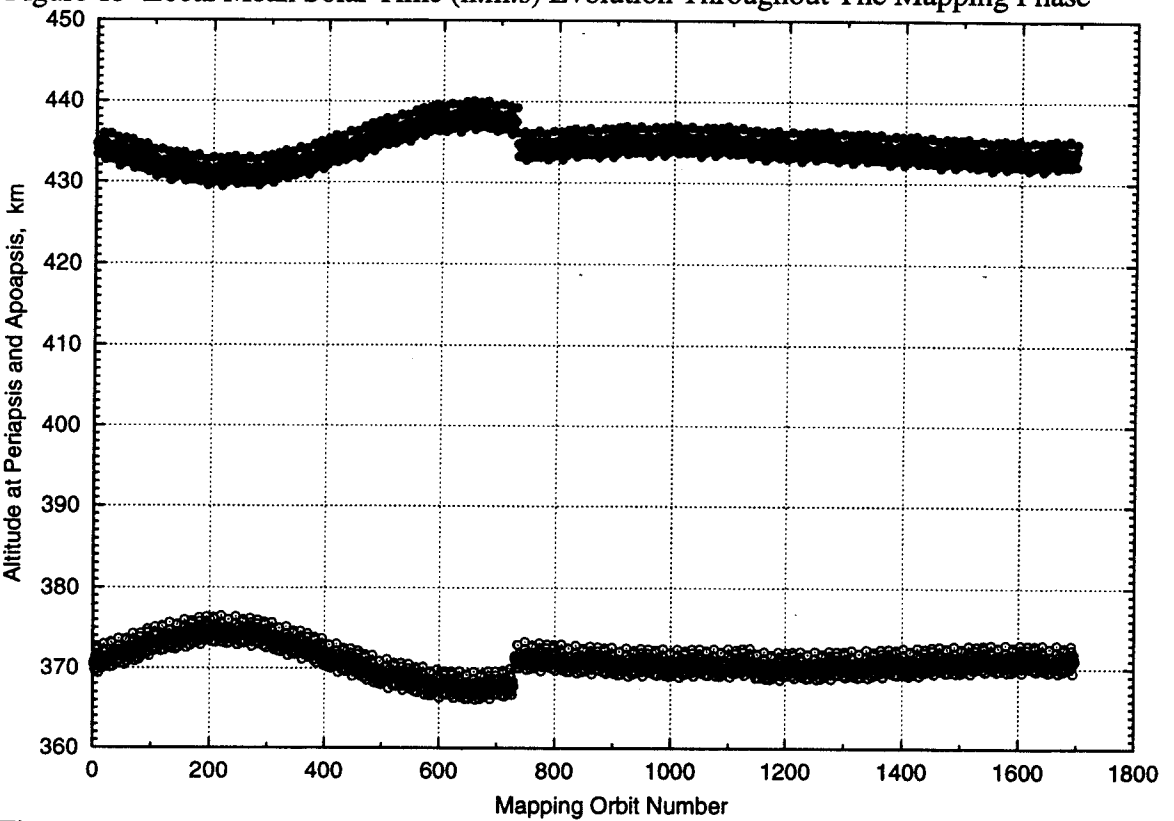

Figure 14 Altitude Variation In The Initial Mapping Orbit And After OTM-1 (Orbit 729) When The Frozen Orbit Was Refined.

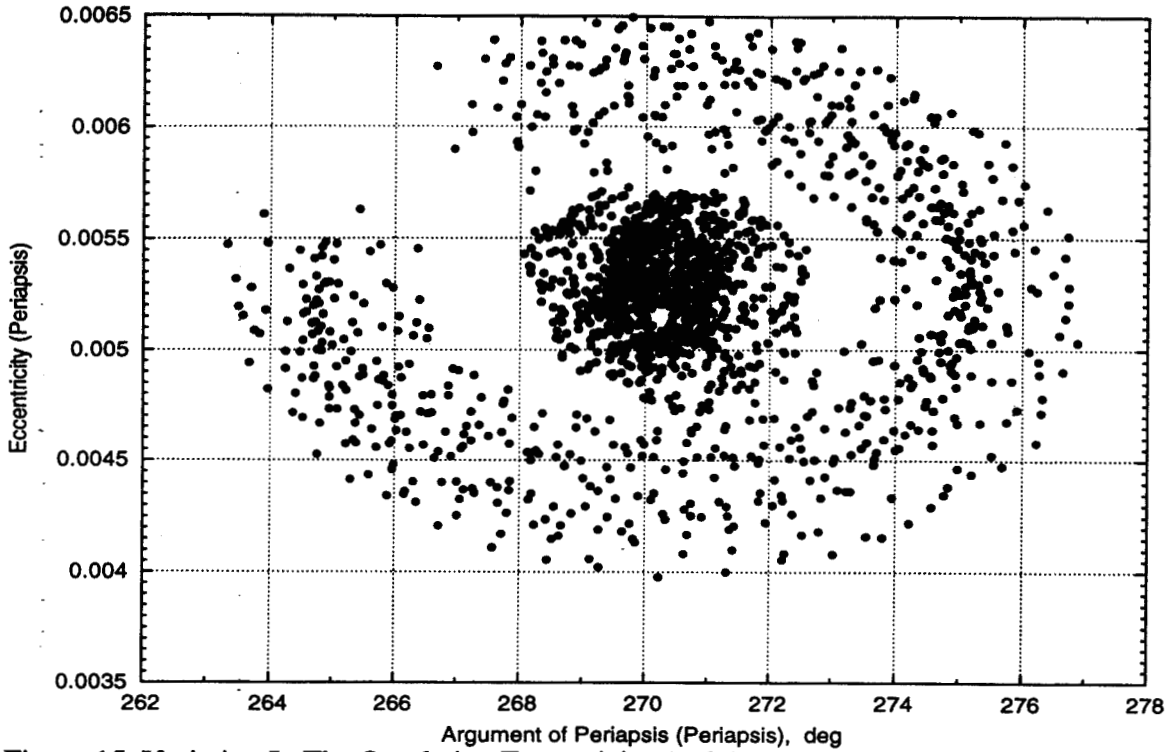

Figure 15 Variation In The Osculating Eccentricity And Argument Of Periapsis Before And After OTM-1.

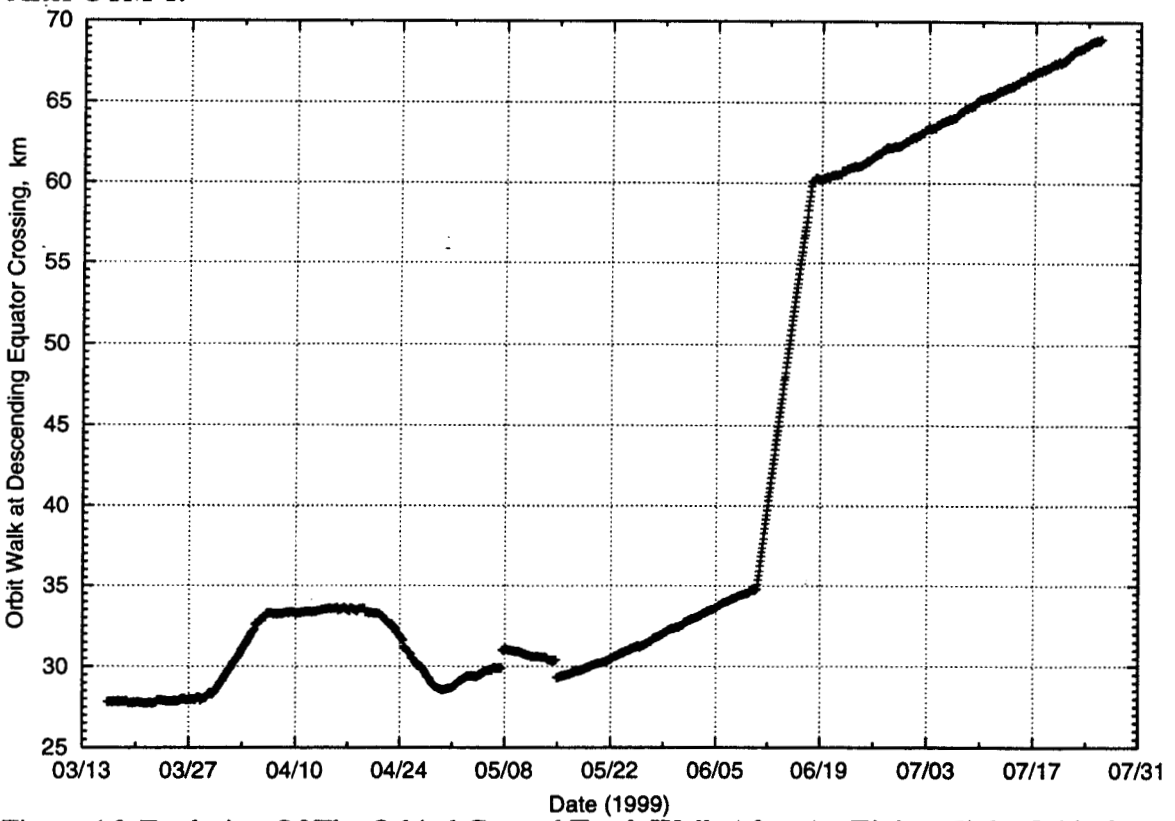

Figure 16 Evolution Of The Orbital Ground Track Walk After An Eighty-Eight Orbit Or A Seven Sol Cycle

On 3/29/99, MGS deployed its HGA which resulted in a series of orbital perturbations which caused the GTW to increase to approximately 34 km thereafter remaining constant for several weeks. On 4/15/99, the spacecraft went into contingency mode due to a HGA azimuth gimbal problem (Ref. 8). This, together with the HGA testing activities over the next week, caused the change of the GTW as shown. Previous to this anomaly, the HGA was put into a stowed or parked position during non contact periods with the Deep Space Network (DSN) in order to minimize gravity gradient forces acting on the spacecraft. Because of the gimbal anomaly, the HGA parked position strategy was no longer feasible. Since that time, there has been an increase in the number of autonomous AMDs executed per day. These orbital perturbations are the most likely cause for the GTW rate of 7.25 km over thirty days as compared to previously being constant. OTM-2, executed on 6/10/99, established a desirable GTW of approximately 60.1 km as shown. However, the GTW rate is still being maintained by the AMDs. The purpose of OTM-3 is to reset the GTW near 50 km and let it drift to approximately 80 km assuming the walk-rate continues as shown in Fig. 16.

ACKNOWLEDGMENT

The work described in this paper was performed at the Jet Propulsion Laboratory, California Institute of Technology, under contract with the National Aeronautics and Space Administration.

The Navigation Team gratefully acknowledges the support and interaction with many members of the MSOP flight team, both at JPL and the Lockheed Martin Astronautics facility at Denver, CO, the Atmospheric Advisory Group especially the George Washington University Group located at Langley Space Flight Center and the Deep Space Network for acquisition of tracking data.

REFERENCES

1. M. D. Johnston et al, "Mars Global Surveyor Aerobraking at Mars," AAS/AIAA Space Flight Mechanics Meeting, Paper AAS 98-112, Monterey, CA, 9-11 Feb 1998.

2. P. Esposito et al, "Mars Global Surveyor: Navigation and Aerobraking at Mars," Proceedings of the 13th International Symposium on Space Flight Dynamics, Goddard Space Flight Center, Greenbelt, Md, May 11-15,1998.

3. C. G. Justus et al, "A Revised Thermosphere for the Mars Global Reference Atmospheric Model (Mars-GRAM Version 3.4)," NASA Technical Memorandum 108513, Marshall Space Flight Center, July, 1996.

4. A. Konopliv and W. Sjogren, "The JPL Mars Gravity Field, Mars 50c, Based Upon Viking and Mariner 9 Doppler Tracking Data," JPL Publication 95-5, Feb 1995.

5. M. E. Davies et al, "Report of the IAU/IAG/COSPAR Working Group on Cartographic Coordinates and Rotational Elements of the Planets and Satellites: 1991",

Celestial Mechanics and Dynamical Astronomy 53, 377-397, 1992.

6. M. D. Johnston et al, "The Strategy for the Second Phase of Aerobraking Mars Global Surveyor," AAS/AIAA Astrodynamics Specialists Conference, Paper AAS 99-303, Girdwood, Alaska, 16-19 August 1999.

7. C. Uphoff, "Orbit Selection for a Mars Geoscience/Climatology Orbiter", AIAA Paper 84-0318, Jan. 1984.

8. B. Smith, "Antenna Problem Stalls Mars Mapping Mission," Aviation Week and Space Technology, p. 85, 26 April 1999.